Study on Bearing Impedance Properties at Several Hundred Kilohertz for Different Electric Machine Operating Parameters

Ville Niskanen, Annette Muetze, *Senior Member, IEEE*, and Jero Ahola

***Abstract*—The possibility of bearing damage caused by inverter-induced bearing currents in modern variable-speed drive systems has been well recognized. However, the breakdown and current conduction mechanisms have still not been well understood today. We present results on the HF impedance properties of rolling element bearings at 300-kHz and 1.5-MHz signals—frequencies taken from the typical spectra of HF circulating bearing currents. Different motor speeds, bearing temperatures, voltages across the bearing, and two different motor sizes are investigated. Notably, we analyze the frequency of transitions between ohmic and capacitive behavior (or vice versa)—the "mode transitions"—as a function of these operating parameters: For some operating conditions, the bearing impedance alternates between capacitive and ohmic behavior without any modification of the macroscopic conditions it is subjected to.**

***Index Terms*—Bearings (mechanical), condition monitoring, variable-frequency drives.**

NOMENCLATURE

BVR	Bearing voltage ratio.
CM	Common mode.
DE	Drive-end.
DFT	Discrete Fourier transform.
HF	High frequency.
NDE	Nondrive-end.
RF	Radio frequency.
TRA	Transition activity.
C_b	Bearing capacitance.
i_b	Bearing current.
i_{CM}	CM current.
F_s	Frequency of HF supply voltage.
$R_{b,\min}$	Minimum bearing resistance.
v_b	Voltage across bearing.
v_{CM}	CM voltage.
Z_b	Bearing impedance.

Manuscript received September 19, 2013; revised January 2, 2014; accepted February 3, 2014. Date of publication February 26, 2014; date of current version September 16, 2014. Paper 2013-IDC-682.R1, presented at the 2013 IEEE Energy Conversion Congress and Exposition, Denver, CO, USA, September 16–20, and approved for publication in the IEEE TRANSACTIONS ON INDUSTRY APPLICATIONS by the Industrial Drives Committee of the IEEE Industry Applications Society.
V. Niskanen and J. Ahola are with Lappeenranta University, 53850 Lappeenranta, Finland (e-mail: ville.niskanen@lut.fi; jero.ahola@lut.fi).
A. Muetze is with Graz University of Technology, 8010 Graz, Austria (e-mail: muetze@tugraz.at).
Color versions of one or more of the figures in this paper are available online at http://ieeexplore.ieee.org.
Digital Object Identifier 10.1109/TIA.2014.2308392

I. MOTIVATION

THE possibility of bearing damage caused by inverter-induced bearing currents in modern variable-speed drive systems has been well recognized. Different authors have described the cause-and-effect chains, allowing the selection of appropriate mitigation techniques (e.g., [1]–[8]). Notably, the distinction between 1) discharge bearing currents, which are directly related to the high-frequency (HF) common-mode (CM) voltage, and 2) HF circulating current that are caused by inductive coupling by the HF stator CM current and that are thus more prevalent with machines with larger frame sizes is important.

Occurrence or prevalence of one or another bearing current type as a function of the machine operating conditions has been described. These are closely related to the respective properties of the bearing impedance, i.e., if the bearing behaves mainly electrically insulating or conducting. In the first case, it is generally represented as a capacitor with capacitances ranging between some hundred picofarads and a few tens of nanofarads [9]–[13]. In the latter case, the bearing is represented as a resistance of a few milliohms [14] (deriving the behavior from [15]).

Some individual results have been presented, aiming to better understand the damage mechanisms within the bearing and the bearing current flow itself. These include analysis of the repetition rate, melting and vaporization levels, discharge energies, and differences of the change of running surface properties for different types of currents, e.g., [16]–[20].

However, the breakdown mechanism when an electrically insulating capacitively behaving bearing loses its electrically insulating properties and a breakdown occurs has still not been well understood today. Furthermore, the current understanding of the current conduction mechanisms through a bearing that is described to behave ohmic is only fairly macroscopic. Neither the moment current flow through a given bearing begins, nor the conduction and, thus, the origin of the resistance on a microscopic scale are well understood.

II. OVERVIEW OF THIS PAPER

We present results on the HF impedance properties of rolling element bearings at 300-kHz and 1.5-MHz signals—frequencies taken from the typical spectra of HF circulating bearing currents (note that here the term "HF" is used to describe relatively high frequencies from an electric machines' perspective but that these frequencies are still low for the field of radio frequency (RF) engineering). Different motor speeds, bearing temperatures, voltages across the bearing, and two different motor sizes, namely, 160 and 280 mm, are investigated. Notably, we analyze the frequency of transitions between ohmic and capacitive behavior (or vice versa)—the "mode transitions"—as a function of these operating parameters: For some operating conditions, the bearing impedance alternates between capacitive and ohmic behavior without any modification of the macroscopic conditions it is subjected to.

The results will contribute to a better understanding of the previously described breakdown and current conduction mechanisms, notably relating to HF circulating bearing currents. This will eventually lead to improved capabilities to assess the risk a certain drive might suffer from bearing failure due to HF inverter-induced bearing currents—notably due to HF circulating bearing currents on which much less has been written than on discharge bearing currents—and to decide on the need of mitigation techniques to be applied.

Our analysis is based on experimental results obtained with two machines with different frame sizes that we support with theoretical considerations. Following a short review of the two HF bearing current types referred to, the discharge and the HF circulating bearing currents, and brief presentations of the test setups including the measurement technique, we discuss the bearing mode transition phenomena and how it changes with electric machine motor speed, bearing temperature, and voltage the bearing is subject to.

III. Review: Discharge Versus HF Circulating Bearing Currents

A. HF Bearing Current Mechanisms

The nonzero HF CM at the output of modern fast-switching inverters typically changes with every inverter switching instant. If no additional measures (such as filters or special control schemes) are applied, it arrives at the motor terminals with a high dv/dt, where it interacts with the HF machine impedance. As a result of this interaction, an HF CM current might flow, which has already been the topic of numerous works. The frequencies of these currents are typically in the range of a few hundred kilohertz, with the first half-period of the oscillation sometimes reaching 1–2 MHz. Some types of HF bearing currents are caused by this HF CM current. Others are directly caused by the HF CM voltage and are fairly independent of any HF CM current. Discharge bearing currents belong to the latter, and HF circulating currents belong to the first group (Fig. 1).

1) *Discharge bearing currents* result from the stator winding HF CM voltage charging the bearings via a capacitive voltage divider (the so-called "bearing voltage ratio" (BVR), e.g., [9] and [10]). They occur—statistically distributed—as discharge current pulses (of up to a few amperes) when the threshold voltage of the bearings (that depends on the operating conditions and typically is in the range of a few up to some tens of volts) is exceeded.

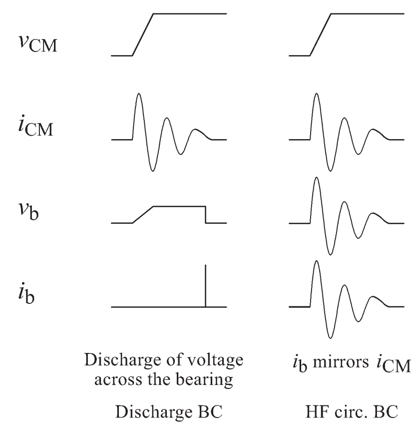

Fig. 1. Comparison of discharge and HF circulating bearing current mechanisms: discharge of capacitively coupled CM voltage across the bearing versus inductive coupling; v_{CM}: CM voltage, i_{CM}: CM current, v_b: voltage across bearing, i_b: bearing current.

2) *HF circulating bearing currents* are caused by inductive coupling through the HF stator CM current and thus mirror the HF CM current. Such currents occur (with amplitudes between a few and more than tens of amperes, depending mostly on the machine size and grounding configuration) the moment a switching event takes place and an HF CM current is generated.

Other bearing current types that have been classified include small capacitive displacement currents as well as HF bearing currents due to rotor ground currents. The first is generally considered to not put the bearing at risk. The latter shows similar current waveforms as the HF circulating bearing currents and is thus not referred to separately in the following discussions.

B. Bearing Impedance Properties

At large, the properties of the bearing impedance when different HF bearing currents flow have been classified as follows.

1) When discharge bearing currents occur, the bearing acts as a capacitance ranging between some hundred picofarads and a few tens of nanofarads [9]–[13]. This capacitance is short circuited (breakdown within the bearing) with a certain probability. The likeliness for a discharge to occur strongly depends on the different operating conditions of the machines, notably the rotational speed of the motor [12], the voltage occurring across the bearing due to capacitive coupling, and the time the bearing has been operating [22].
2) When HF circulating currents flow, the bearings show mainly ohmic behavior. The increase of such currents with decreasing motor speed is explained by smaller bearing impedances at lower motor speed. However, the bearing resistance is generally considered negligibly small when compared to the remaining impedances of the HF bearing current path through the machine stator lamination stack, end shields, and rotor [14].

Neither the mechanisms taking place the moment HF circulating currents start to flow nor the breakdown mechanism of discharge bearing currents is well understood today.

IV. Test Setup

A. Drive Systems

Two three-phase, 230/400-V, 50-Hz, Δ-connected, and four-pole induction motors of two different power levels, referred to as "motor MA-15" and "MB-75," were used for the experimental analysis. Motor MA-15 is a 160-mm frame size 15-kW machine, and MB-75 is a 280-mm frame size 75-kW machine. Motor MA-15 has 6309 C3, and motor MB-75 has 6316 C3 bearings. All bearings are from the same manufacturer and have been greased with a multipurpose grease for industrial applications (Shell Alvania RL2).

The two motors were operated at no load by two three-phase 400-V 50-Hz inverters, referred to as "inverter IA-15" and "inverter IB-75," respectively. Inverter IA-15 is rated at 14.8 A and is operated at 4 kHz (scalar control and constant switching frequency). Inverter IB-75 is rated at 82 A and is operated at 3 kHz (direct torque control and average switching frequency). The inverters are only used to control the speed of the machines. As discussed in the following section, their types and control schemes do not influence the measurement results and their analysis.

B. Measurement Technique

Fig. 4 illustrates the measurement technique applied, including the bearing insulation, placement of current and voltage probes, and external HF voltage supply.

Both bearings of the machines were insulated toward the housing using an electrically insulating layer (polyethene) of 5 mm thickness applied around the outer bearing race. The nondrive-end (NDE) bearing insulations were left open so that any current flow across the NDE bearing could be considered negligible: Even at 1 MHz, the impedance provided by the electrically insulating layer is on the order of several kiloohms, which is at least by a factor of 10^3 larger than the one of the bearing current path.

The insulations around the drive-end (DE) bearings were short circuited with a short wire to measure the HF bearing currents flowing through the DE bearings. The HF bearing currents were measured with a Tektronix TCP202 50 MHz (MA-15) respective R&S RT-ZC20 100 MHz (MB-75) current, and the voltage across the bearing was measured with a Tektronix P5210 50 MHz (MA-15) respective R&S RT-ZD01 100 MHz (MB-75) high-voltage differential probe (Figs. 2–4).

The DE bearings were submitted to externally supplied HF ac voltages of $F_s = 300$ kHz and 1.5 MHz using a Hameg HM8131-2 15 MHz signal generator (output impedance of 50 Ω). These frequencies are in the range typical for HF circulating bearing currents. Any current flowing through the bearing would thus result from a breakdown occurring within the bearing and the bearing being in conductive (resistive) mode. Note that this external voltage occurs in parallel to the bearing and rotor-to-frame capacitance of the BVR capacitive voltage divider. Solving for the voltage across the bearing through the law of superposition, the voltage across the bearing is thus determined by the externally supplied voltage $U_{b,\mathrm{ext}}$ and with the influence of the feeding inverter negligible.

Fig. 2. Measurement setup of motor MA-15 (15 kW).

Fig. 3. Measurement setup of motor MB-75 (75 kW).

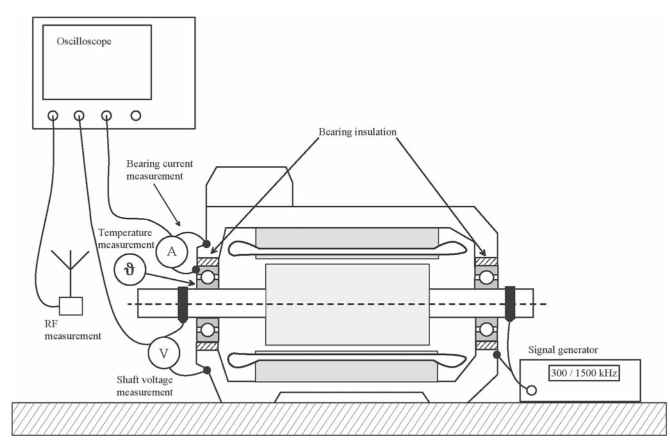

Fig. 4. Measurement technique.

Both for the HF voltage supply and for the voltage measurement, the shaft was contacted with the help of a sleeve made from the tinned copper braid of a coaxial shield of a supply cable, providing a relatively large contact area of almost 11 cm^2. The shaft surface was further polished with fine sandpaper, and an additional weight of around 200 g was attached to the sleeve to further improve the contact.

A discrete Fourier transform (DFT) was applied to the recorded DE bearing voltage and current signals to compute the bearing capacitance C_b and minimum bearing resistance $R_{b,\min}$ corresponding to the two modes of conduction (capacitive/resistive behavior), respectively. While the minimum bearing resistance $R_{b,\min}$ is a fixed point value, the bearing capacitance C_b was computed from the averaged values over the respective recorded time window; $C_b = \text{ave}\{1/(2\pi F_s|Z_b|)\}$, with Z_b computed from the measured voltage across and current through the bearing.

Bearing temperatures changed over time as the motor was operated and were measured using an AZ8868 infrared thermometer between the motor shaft and DE end shield (uncertainty estimated to $\pm 5°$).

V. Observation: Bearing Impedance Mode Transitions

As per the conventional classification of the bearing impedance properties described previously (Section III-B), a bearing shows either ohmic or capacitive behavior. The operating conditions of the drive and, thus, of the bearing mostly determine this characteristic. Strictly speaking, it would be more appropriate to say that a bearing shows "mainly" or "most likely" one or the other behavior.

Transition from capacitive to ohmic behavior has been mostly associated with voltage building up across a bearing followed by a subsequent breakdown, such as in the case of discharge bearing currents. In such cases, the voltage across the bearing would be reduced to the voltage drop at the bearing internal resistance due to any bearing current flow, and the bearing remains conductive until the current flow has decayed. Then, voltage might build up again across the bearing, e.g., due to capacitive coupling, as in the case of discharge currents.

Concerning HF voltages in the range of a few hundred kilohertz, which are at the origin of HF circulating bearing currents, we have recently shown that there is a time difference between the ac voltage occurring across the bearing and the bearing becoming resistive. This makes the application of an RF-based bearing current detection method, such as the one proposed in [23] and [24], possible [25].

In this paper, we further study such nonsteady behavior of the bearing electric characteristics: We show that, for some operating conditions, the bearing impedance alternates between capacitive and ohmic behavior without any modification of the macroscopic conditions it is subjected to.

Exemplarily, Figs. 5 and 6 show the measured bearing currents and voltages of motor MA-15 at 210 r/min motor speed and of MB-75 at 450 r/min, both at 300-kHz HF supply voltage: Within the time-window of observation of 400 μs, the bearing changes three times between resistive and capacitive behavior. The 300-kHz HF voltage (during capacitive behavior) and the HF current flow (during resistive behavior), as well as the discharge current as the bearing changes from capacitive

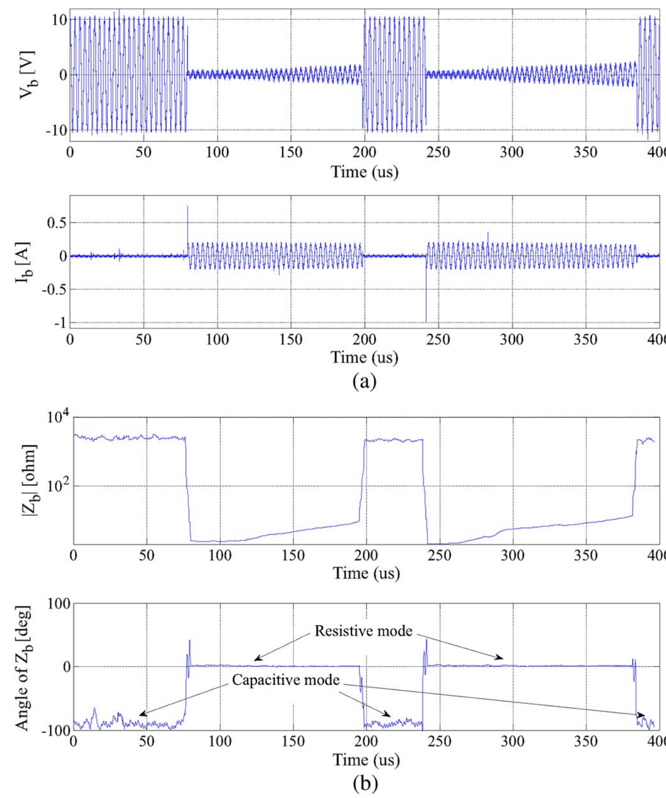

Fig. 5. Motor MA-15 and inverter IA-15: measured currents, voltages, and RF signals and computed bearing impedance for 300-kHz 14-Vpp HF supply voltage and 210-r/min motor speed, with a DE shaft temperature of 32 °C; computed bearing capacitance during capacitive behavior $C_b = 0.29$ nF and $R_{b,\min} = 2.6\ \Omega$. (a) Measured bearing current and bearing voltage. (b) Computed bearing impedance.

to resistive mode, can clearly be seen. The transition from resistive to capacitive mode is preceded by a slight increase of the bearing impedance over a certain time of some tens of microseconds.

Such behavior can be observed for different motor speeds and supply voltages and for both the smaller and larger motors. A methodology was developed to systematically investigate, describe, and quantify the behavior, which is presented in the following.

VI. Methodology: Impedance Mode Transition Analysis

A. Configurations Analyzed

Two frequencies were chosen for the HF supply voltage—300 kHz and 1.5 MHz: The oscillation frequencies of HF circulating bearing currents are typically on the order of a few hundred kilohertz. However, often, the initial current rise is much faster and comprises frequencies between 1 and 2 MHz. The transitions between different bearing modes were analyzed for the following for both the smaller and larger motors:

1) up to 3000-r/min motor speed;
2) HF supply voltages for which a change of bearing impedance mode was observed (between 5 and 20 Vpp); note that there is a lower bound of voltage below which no discharges occur and the bearing behaves capacitively

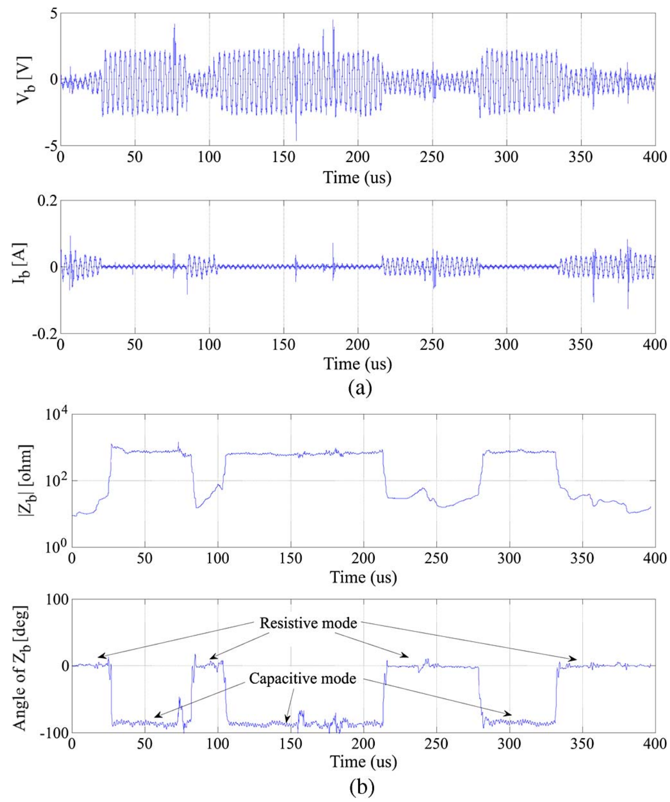

Fig. 6. Motor MB-75 and inverter IB-75: measured currents and voltages and computed bearing impedance for 300-kHz 5-Vpp HF supply voltage and 450-r/min motor speed, with a DE shaft temperature of 44 °C; computed bearing capacitance during capacitive behavior $C_b = 0.83$ nF and $R_{b,\min} = 5.3\ \Omega$. (a) Measured bearing current and bearing voltage. (b) Computed bearing impedance.

only, and there is an upper bound of voltages above which discharges do not occur any longer as the bearing behaves ohmic only (as will be explained in the following);

3) bearing temperatures between 20 °C and close to 70 °C; note that changes of bearing impedance mode were not observed within this whole range, since for elevated bearing temperatures, the bearing is fully conductive (as will also be explained in the following).

B. Transition Activity

To quantify the bearing electric mode transitions, we introduce the notion of "transition activity," TRA. The TRA is computed from the number of transitions from capacitive to resistive mode counted within a certain time window and given in discharges/second. Between two such transitions, a change from resistive to capacitive mode has to occur. These are not counted separately, since they are the requirement for another discharge to occur. Furthermore, the transitions from capacitive to resistive mode are understood to correlate with a discharge that can—provided enough energy is released—be detected through the RF-based detection method.

The TRA is obtained through postprocessing in MATLAB based on envelope detection (demodulation technique from amplitude modulation): In the measurements, 300 kHz is the carrier wave that is modulated by the bearing mode. A hysteresis filter is applied to eliminate noise (thresholds set at 0.7 Vpp for capacitive and 0.3 Vpp for resistive behavior). In our analysis, the TRA was based on measurements taken for time windows of 100 ms taken at a sampling rate of 25 MS/s.

A rather large scattering of the TRA was observed during the measurements, indicating the complex phenomena within the bearing that cannot easily be reproduced by running at the very same motor speed and bearing temperature only again. This is very much in line with the significant scattering of the so-called "discharge activity" observed with discharge bearing currents (see [22]). Therefore, the findings obtained may serve for a qualitative assessment of the influence of the different operating parameters, but any quantitative statement has to be made with caution.

C. P.U. Modes

Furthermore, the relative amount of time during which the bearing is in one or another mode is computed. Thus, the p.u. capacitive mode is obtained from the time—indicated by the number of samples—the bearing shows capacitive behavior divided by the total number of samples within one time window (here, 100 ms, i.e., $2.5 \cdot 10^6$ samples).

D. Bearing Temperature—Speed Line

The observations suggest the derivation of a "bearing temperature—speed line." This line describes the mechanical–electrical interaction inside the bearings and gives—of indicative nature—the bearing temperature required for a certain speed for the bearing to behave fully conducting or, vice versa, the minimum speed required for a given bearing temperature for the bearing to also show electrically insulating behavior.

VII. Motor MA-15: Measured Transition Activities

A. Introduction

Figs. 7–9 show exemplary results for the transition mode analysis of motor MA-15: In Figs. 7 and 8, the voltages and currents have been recorded for two levels of temperature and three levels of HF supply voltage for 240- and 1500-r/min motor speed, respectively. Fig. 9(a) and (b) displays the measured TRA as a function of bearing temperature and motor speed. Aiming to further quantify the findings, Tables I and II show the computed TRAs for selected sets of analyses.

B. Influence of Bearing Temperature

Considering Figs. 7–9, the relative amount of time during which the bearing shows ohmic behavior increases with temperature. This holds true for both motor speeds and all three supply voltages. We explain this behavior by the decreasing thickness of the lubricating film and thus reduced ability to withstand any voltage. Note that the decreasing thickness of the lubricating film is also reflected in the increasing values of the bearing capacitances C_b in Table I.

From Fig. 9(a) and (b), it becomes clear that the TRA only increases with bearing temperature until it suddenly reduces,

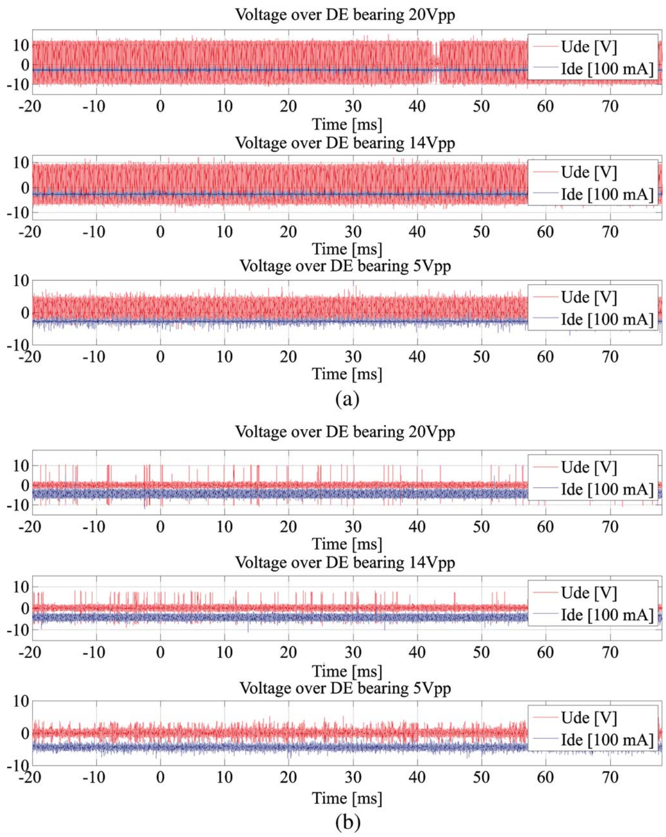

Fig. 7. Motor MA-15 and inverter IA-15—transition mode analysis: measured currents and voltages for 300-kHz HF supply voltage and 420-r/min motor speed; computed bearing capacitance during capacitive behavior $C_b = 0.36$ nF (23 °C) respective $C_b = 0.89$ nF (37 °C). (a) DE shaft temperature of 23 °C. (b) DE shaft temperature of 37 °C.

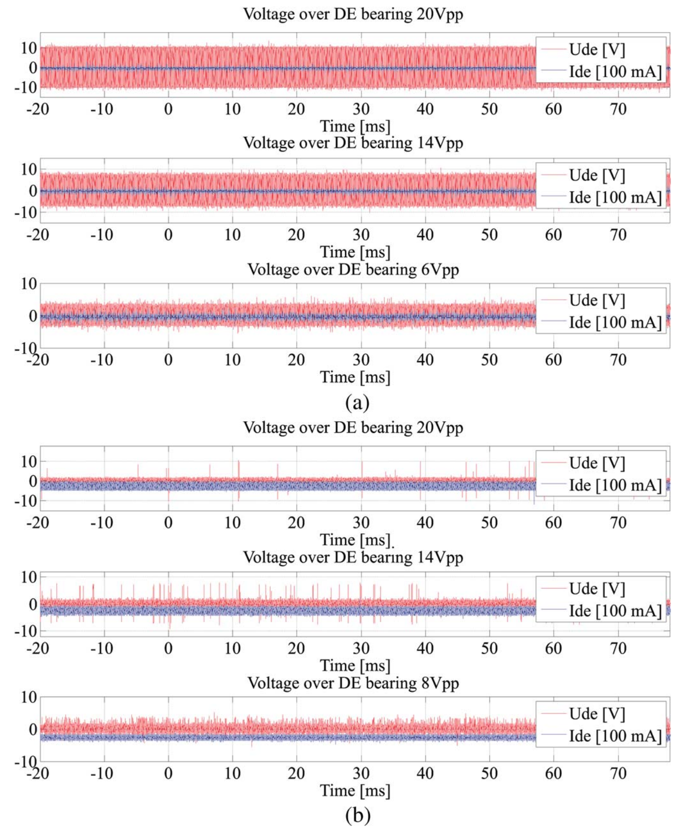

Fig. 8. Motor MA-15 and inverter IA-15—transition mode analysis: measured currents and voltages for 300-kHz HF supply voltage and 1500-r/min motor speed; computed bearing capacitance during capacitive behavior $C_b = 0.62$ nF (both temperatures). (a) DE shaft temperature of 30 °C. (b) DE shaft temperature of 56 °C.

shortly before the bearing becomes fully conductive and transitions have ceased to occur: As of a certain bearing temperature, the relative amount during which the bearing remains conductive increases and its ability to restore capacitive mode decreases. This behavior is also reflected in the numbers shown in Table I.

Fig. 9 also illustrates well the rather large scattering of the aforementioned TRA.

C. Influence of Motor Speed

Comparing Figs. 7 and 8 and considering the numbers shown in Table I, a decrease of the TRA is observed as the motor speed increases. This tendency is again explained by an increase of the thickness of the lubricating film with increasing speed (resulting in decreasing bearing capacitances C_b in Table I).

Here, again, Fig. 9(a) and (b) confirms the general tendency but shows the significant scattering of the measured and thus the variability of the TRA.

D. Influence of HF Supply Voltage

Comparing the subfigures of Fig. 9(a) and (b) for the different bearing temperatures as well as the values listed in Table II reveals contrasting behavior regarding the influence of the HF supply voltage on the TRA: For "lower" bearing temperatures, the TRA increases with the HF supply voltage. As the voltage across the bearing increases, the likeliness the bearing might withstand it decreases. However, for "higher" bearing temperatures, the TRA decreases with the voltage across the bearing. This suggests that the energy released into the bearing (proportional to the square of the voltage across the bearing) influences the ability of the bearing to restore capacitive mode, required for another breakdown to happen.

Furthermore, no remarkable difference between the frequencies of the HF supply voltage, 300 kHz versus 1.5 MHz, is observed from Fig. 9. A slight increase of the TRA might be interpreted from the values shown in Table I, but such interpretation has to be taken with caution because of the variation of the TRA between different sets of measurements. Any difference that might exist (see Section VI-D) is thus understood to be hidden within the scattering of the latter.

VIII. MOTOR MB-75: MEASURED TRANSITION ACTIVITIES

A. Comparison With Behavior of the Smaller Motor MA-15

With the large machine, the bearing is in resistive mode for HF supply voltages above 10 Vpp. Meaningful and convincing results require HF supply voltages well below this limit, for which reason the further analysis only reports on measurements obtained with supply voltages of 5 Vpp.

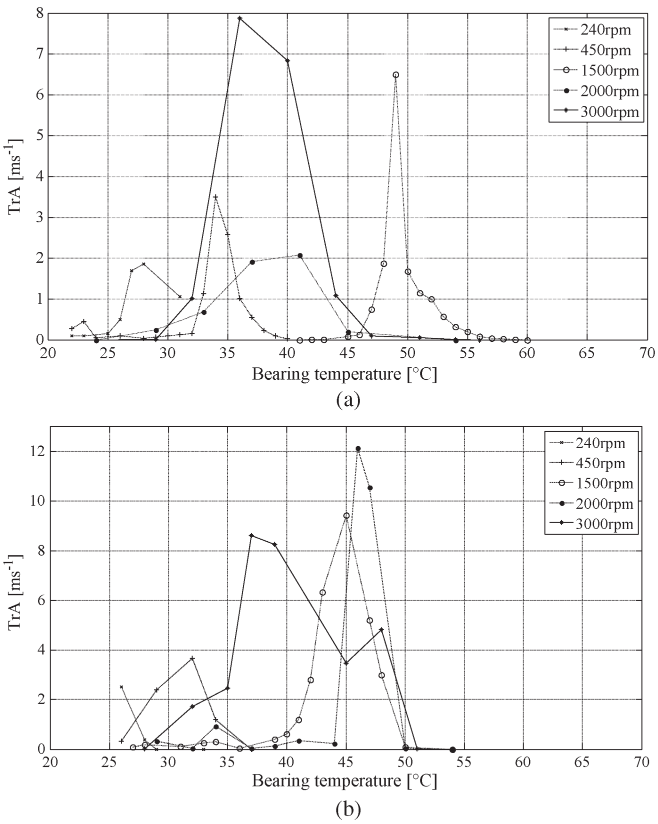

Fig. 9. Motor MA-15 and inverter IA-15: measured transition activity as a function of bearing temperature and motor speed, 5-Vpp HF supply voltage. (a) 300-kHz HF supply voltage. (b) 1.5-MHz HF supply voltage.

When in resistive mode, the bearing impedance is generally larger, and the current flow is smaller than that for the smaller machine (compare also Figs. 5 and 6): The current flow as it occurs when circulating bearing currents are flowing has not fully established itself. Before the current flow has led to the establishment of further current-conducting bridges, the bearing impedance increases again.

Fig. 10 shows the measured bearing voltages and currents for 1.5-MHz HF supply voltage at motor speed as high as 3000 r/min. Within the time window of observation of 400 μs, the bearing impedance changes again three times between capacitive and resistive behavior.

In addition, a third mode that might be described as "RC-behavior" is observed. It occurs as an intermediate stage between mainly resistive and mainly capacitive behavior. This mode is exemplarily illustrated in Fig. 11 (between 140 and 180 μs): The magnitude of the bearing impedance remains high (in the range of 10^3 Ω), but its angle reduces down to around 45°.

In both of these latter cases, the bearing impedance when in resistive mode is on the order of 9 Ω and thus even larger than in the previously shown case (Fig. 6; $R_{b,\min} = 5.3\ \Omega$).

TABLE I
MOTORS MA-15 AND MB-75, 300-kHz AND 1.5-MHz 5-Vpp HF SUPPLY VOLTAGE: COMPUTED TRANSITION ACTIVITY, TrA, CAPACITIVE P.U. MODES, AND BEARING CAPACITANCE DURING CAPACITIVE BEHAVIOR C_b

n [rpm]	Θ [°C]	TrA [ms^{-1}]	Cap. mode [p.u.]	Computed C_b [nF]
Motor MA-15				
300 kHz HF supply voltage				
240	23	0.15	0.9998	0.36
	37	10.08	0.1382	0.89
450	28	0	0.9997	0.36
	48	2.16	0.0328	0.90
1500	30	0	1.0000	0.62
	56	2.44	0.0181	n.a.
2000	24	0	1.0000	0.12
	41	2.08	0.0235	0.31
3000	24	0	1.0000	0.12
	44	1.08	0.0110	0.35
1.5 MHz HF supply voltage				
200	28	0.37	0.0158	0.31
400	26	0.33	0.9733	0.24
1500	27	0.08	0.9973	0.15
	48	2.99	0.0478	0.24
2000	29	0.33	0.991	0.14
	47	10.55	0.2491	0.22
3000	28	0.02	0.9992	0.14
	48	4.82	0.0601	0.26
Motor MB-75				
300 kHz HF supply voltage				
240	24	0.27	0.9153	0.51
	37	2.10	0.0713	0.67
450	24	0.26	0.9784	0.36
	37	2.18	0.7782	0.62
	46	3.75	0.1312	0.97
1500	24	0.01	0.9989	0.26
	37	2.79	0.8734	0.51
	57	4.54	0.0556	0.92
2000	27	0	1	0.25
	36	2.63	0.9341	0.32
	47	16.88	0.2757	0.36
3000	28	1	0.9992	0.18
	36	0.45	0.99	0.23
	50	8.55	0.5318	0.40
1.5 MHz HF supply voltage				
200	25	1	0.9985	0.22
400	25	0	1	0.18
	39	4.40	0.2053	0.39
1500	26	0	1	0.18
	39	1.00	0.9997	0.25
	48	6.41	0.643	0.54
2000	27	0	1	0.16
	50	6.80	0.159	0.55
	64	0.50	0.001	1.10
3000	28	0.04	0.9985	0.20
	38	4.65	0.8651	0.26
	50	10.00	0.6378	0.40

B. Influence of Bearing Temperature, Motor Speed, and HF Supply Voltage: Further Comments

The lower capability to withstand voltage, higher bearing impedance in resistive mode, and existence of an "intermediate" stage are the main differences observed when compared with the smaller machine. The observations regarding the influences of the bearing temperature, motor speed, and HF supply voltage on the TrA are very similar to those made with motor MA-15.

TABLE II

MOTOR MA-15, 300-KHZ HF SUPPLY VOLTAGE: COMPUTED TRANSITION ACTIVITY, TRA, RELATIVE AMOUNT OF TIME OF CAPACITIVE BEARING BEHAVIOR, AND COMPUTED BEARING CAPACITANCE DURING CAPACITIVE BEHAVIOR FOR DIFFERENT AMPLITUDES OF THE SUPPLY VOLTAGE

n [rpm]	Θ [°C]	TRA [ms^{-1}] 20 Vpp	14 Vpp	5 Vpp	Cap. mode [p.u.] 20 Vpp	14 Vpp	5 Vpp	Computed C_b [nF]
240	23	3.71	0.25	0.15	0.9699	0.9999	0.9998	0.36
	37	1.44	2.24	10.08	0.0091	0.0247	0.1382	0.89
450	28	0.02	0	0	0.9999	0.9999	0.9997	0.36
	48	0.12	0.10	2.16	0.0004	0.0008	0.0328	0.90
1500	30	0	0	0	1.0000	1.0000	1.0000	0.62
	56	0.19	0.48	2.44	0.0006	0.0003	0.0181	n.a.

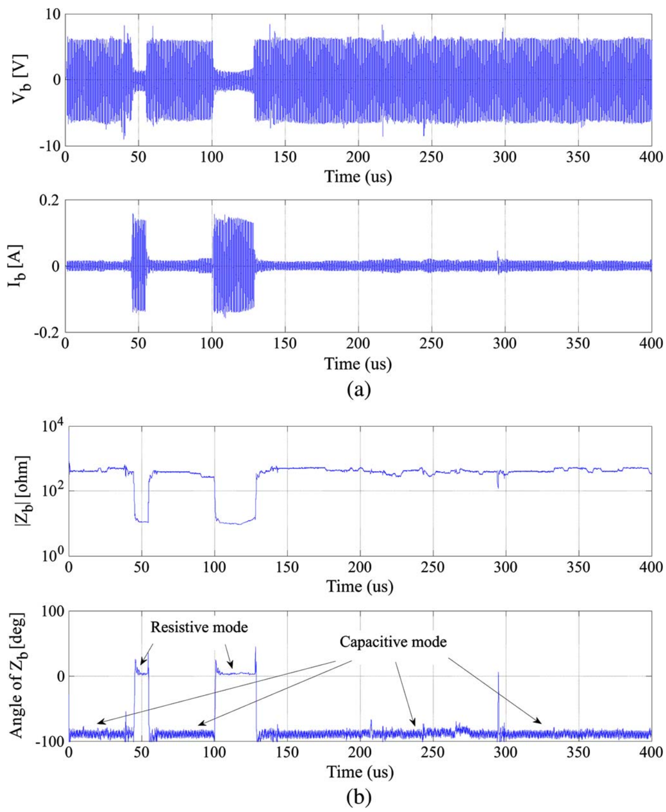

Fig. 10. Motor MB-75 and inverter IB-75: measured currents and voltages and computed bearing impedance for 1.5-MHz 5-Vpp HF supply voltage and 3000-r/min motor speed, with a DE shaft temperature of 32 °C; computed bearing capacitance during capacitive behavior $C_b = 0.26$ nF and $R_{b,\mathrm{min}} = 9.2\ \Omega$. (a) Measured bearing current and bearing voltage. (b) Computed bearing impedance.

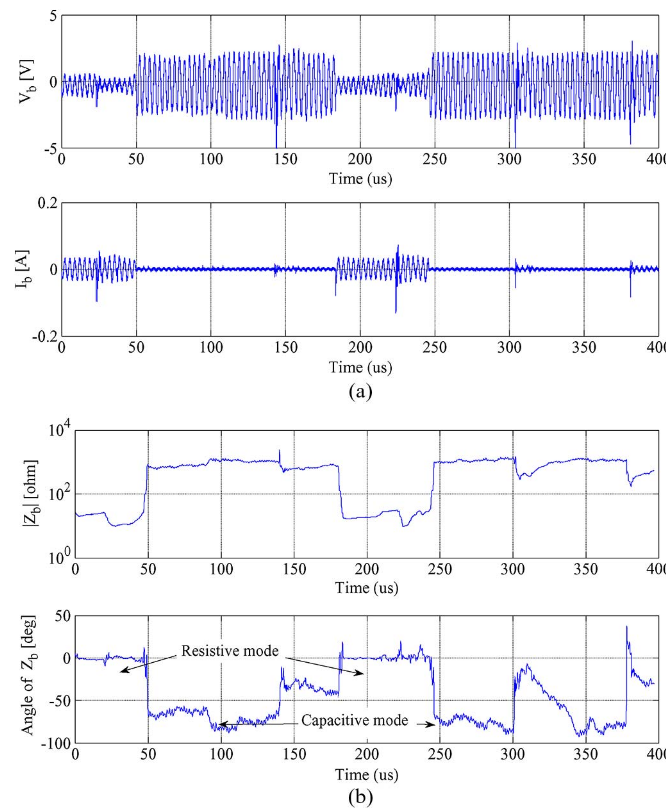

Fig. 11. Motor MB-75 and inverter IB-75: measured currents and voltages and computed bearing impedance for 300-kHz 5-Vpp HF supply voltage and 240-r/min motor speed, with a DE shaft temperature of 37 °C; computed bearing capacitance during capacitive behavior $C_b = 0.67$ nF and $R_{b,\mathrm{min}} = 9.0\ \Omega$. (a) Measured bearing current and bearing voltage. (b) Computed bearing impedance.

Fig. 12 shows the transition mode analysis of motor MB-75 for a bearing temperature of 37 °C and three different motor speeds. The figures illustrate well how the bearing is more able to withstand the ac voltage with increasing motor speed.

In analogy to Fig. 9, Fig. 13(a) and (b) shows the measured TRAs as a function of bearing temperature and motor speed for motor MB-75. The tendencies shown are the same as with motor MA-15: increasing TRA with increasing bearing temperature until a sudden reduction occurs shortly before the bearing becomes fully conductive, decreasing TRA with increasing motor speed, and a large scattering of the TRA. These findings are also reflected by the values shown in Table I.

In contrast to the results for the smaller motor MA-15 shown in Fig. 9, Fig. 13 shows a general shift of the curves to higher bearing temperatures for 1.5 MHz when compared to 300-kHz HF supply voltage for the larger motor MB-75. These are also reflected in the values shown in Table I, which, however, have again to be taken with caution.

IX. BEARING TEMPERATURE–SPEED LINE

The temperature-speed lines have been derived for both motors and HF supply voltages and are shown in Fig. 14: The threshold values are generally shifted to higher bearing temperatures for the larger when compared with the smaller motor. The influence of the supply voltage is smaller, with the threshold voltages for 1.5 MHz at high bearing temperatures than those occurring with 300-kHz HF supply voltages. It

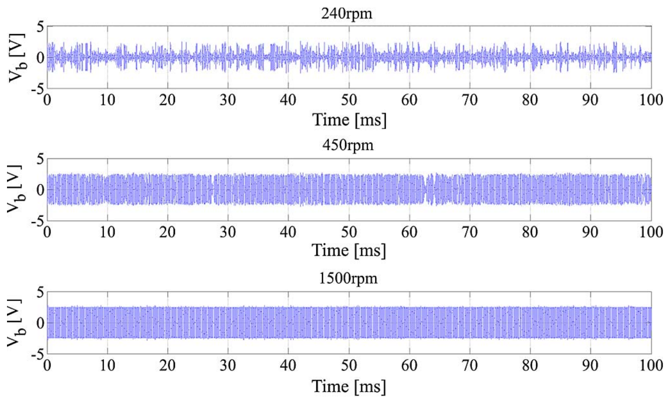

Fig. 12. Motor MB-75 and inverter IB-75—transition mode analysis: measured voltages for three different motor speeds; 300-kHz 5-Vpp HF supply voltage; computed bearing capacitances during capacitive behavior $C_b = 0.67$ (240 r/min), 0.62 (450 r/min), and 0.51 nF (1500 r/min), respectively.

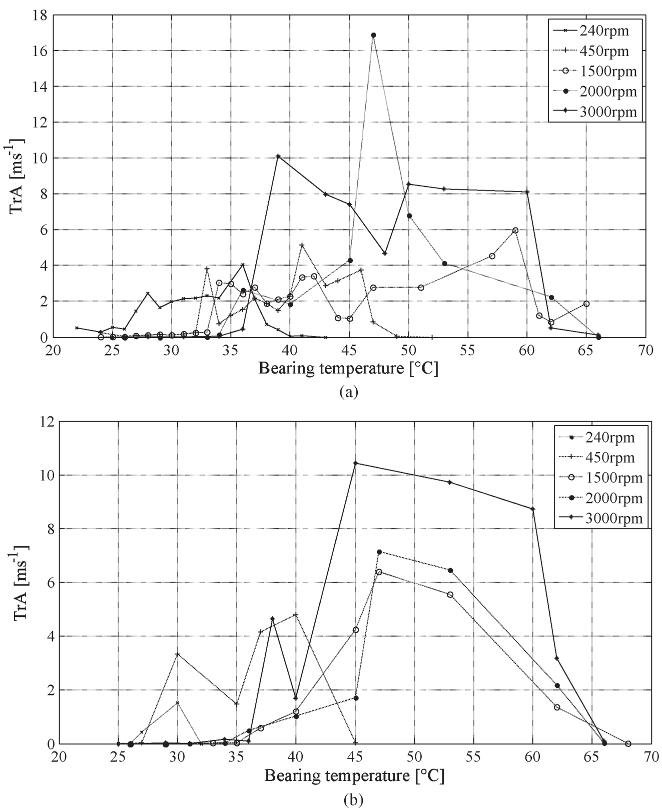

Fig. 13. Motor MB-75 and inverter IB-75: measured transition activity as a function of bearing temperature and motor speed, 5-Vpp HF supply voltage. (a) 300-kHz HF supply voltage. (b) 1.5-MHz HF supply voltage.

should be mentioned again that these lines are of qualitative nature only: In theory, the probability for discharge bearing currents to occur is zero for the area TrA $= 0$. However, considering the scattering of the results discussed previously, any absolute quantitative readings have to be taken with caution.

X. Computed P.U. Modes

In addition to the computed TrAs, Table I shows the p.u. capacitive modes.

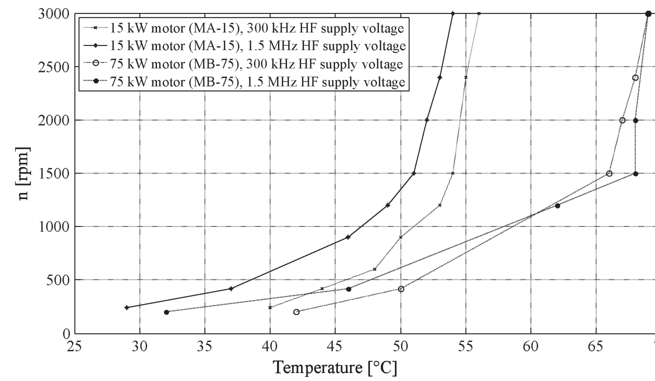

Fig. 14. Bearing temperature—speed line for resistive mode of motors MA-15 and MB-75: speed required for a certain bearing temperature for voltage to build up across the bearing. Below this speed, the bearing behaves resistive. 300-kHz 5-Vpp as well as 1.5-MHz 5-Vpp HF supply voltage.

The behavior observed for the p.u. capacitive modes is analog to the one of the TrA.

1) For a given temperature, the p.u. capacitive mode increases with motor speed as less transitions between capacitive and resistive modes occur.
2) The p.u. capacitive mode decreases with increasing bearing temperature as more transitions between capacitive and resistive modes occur.
3) With respect to the HF supply voltage, the behavior seems to follow the same trends as the TrA.

XI. Conclusion

The current conduction and voltage breakdown mechanism within rolling element bearings is only partially understood today. Further research (ideally using a custom-designed bearing test rig) is needed, eventually aiming for a better understanding of the bearing damage mechanism due to HF bearing currents. Several results on the impedance properties of rolling element bearings under 300 kHz and 1.5 MHz voltage for different motor speeds and bearing temperatures have been presented, and the notion of "mode transitions" has been introduced: For some operating conditions, the bearing impedance alternates between capacitive and ohmic behaviors without any modification of macroscopic conditions the bearing is subjected to. In addition, a third "intermediate" stage in which the bearing impedance remains high but the angle is reduced to about 45° is observed.

Similar to the "discharge activity" that might be used to quantify the occurrence of discharge bearing currents, the number of transitions between different modes—referred to here as TrA—also shows a rather large scattering between individual sets of measurements. Thus, when discussing such TrA, it is advisable to pay attention to general tendencies rather than absolute quantitative values. The TrA has been found to generally increase with bearing temperature and amplitude of HF supply voltage the bearing was subjected to—very much in analogy to the behavior observed with discharge bearing currents.

A "bearing temperature—speed line" can be derived to describe the minimum speed required for a given bearing temperature for the bearing to not only show purely ohmic but also electrically insulating behavior. These threshold values are generally shifted to higher bearing temperatures for the larger when compared with the smaller motor and—but to a smaller extent—for 1.5-MHz instead of 300-kHz HF supply voltages.

Understanding the prevalence of one or the other property, likeliness, and frequency of transition will help to better understand the likeliness of discharge currents to occur and/or of a machine to be able to withstand HF voltage that drives HF circulating bearing currents. The results also indicate that the flow of HF circulating currents might be accompanied by discharges within the bearing, even though not as obvious to be observed externally as those of discharge bearing currents.

ACKNOWLEDGMENT

Funding for the Open Access publication of this paper was provided by the Government of Styria, Department of Science and Health.

REFERENCES

[1] S. Chen, T. A. Lipo, and D. Fitzgerald, "Modeling of bearing currents in inverter drives," *IEEE Trans. Ind. App.*, vol. 32, no. 6, pp. 1365–1370, Nov./Dec. 1996.

[2] S. Chen and T. A. Lipo, "Source of induction motor bearing currents caused by PWM inverters," *IEEE Trans. Energy Convers.*, vol. 11, no. 1, pp. 25–32, Mar. 1996.

[3] P. Link, "Minimizing electric bearing currents in ASD systems," *IEEE Ind. Appl. Mag.*, vol. 5, no. 4, pp. 55–66, Jul./Aug. 1999.

[4] H. E. Boyanton and G. Hodges, "Bearing fluting," *IEEE Ind. Appl. Mag.*, vol. 8, no. 5, pp. 53–57, Sep./Oct. 2002.

[5] R. F. Schiferl and M. J. Melfi, "Bearing current remediation options," *IEEE Ind. Appl. Mag.*, vol. 10, no. 4, pp. 40–50, Jul./Aug. 2004.

[6] A. Muetze and A. Binder, "Don't lose your bearings—Mitigation techniques for bearing currents in inverter-supplied drive systems," *IEEE Ind. Appl. Mag.*, vol. 12, no. 4, pp. 22–31, Jul./Aug. 2006.

[7] A. Muetze and A. Binder, "Practical rules for assessment of inverter-induced bearing currents in inverter-fed ac motors up to 500 kW," *IEEE Trans. Ind. Electron.*, vol. 54, no. 3, pp. 1614–1622, Jun. 2007.

[8] A. Binder and A. Muetze, "Scaling effects of inverter-induced bearing currents in ac machines," *IEEE Trans. Ind. Appl.*, vol. 44, no. 3, pp. 769–776, May/Jun. 2008.

[9] D. Busse, J. Erdman, R. Kerkman, and D. Schlegel, "Bearing currents and their relationship to PWM drives," *IEEE Trans. Power Electron.*, vol. 12, no. 2, pp. 243–252, Mar. 1997.

[10] D. Busse, J. Erdman, R. Kerkman, D. Schlegel, and G. Skibinski, "System electrical parameters and their influence effect on bearing currents," *IEEE Trans. Ind. Appl.*, vol. 33, no. 2, pp. 577–584, Mar./Apr. 1997.

[11] A. Muetze and A. Binder, "Calculation of motor capacitances for prediction of the voltage across the bearings in machines of inverter-based drive systems," *IEEE Trans. Ind. Appl.*, vol. 43, no. 3, pp. 665–672, May/Jun. 2007.

[12] E. Wittek *et al.*, "Capacitances and lubricant film thicknesses of motor bearings under different operating conditions," in *Proc. 14th ICEM*, Rome, Italy, Sep. 6–8, 2010, pp. 1–6.

[13] E. Wittek *et al.*, "Capacitance of bearings for electric motors at variable mechanical loads," in *Proc. 15th ICEM*, Marseille, France, Sep. 2–5, 2012, pp. 1602–1607.

[14] A. Muetze and A. Binder, "Calculation of circulating bearing currents in machines of inverter-based drive systems," *IEEE Trans. Ind. Electron.*, vol. 54, no. 2, pp. 932–938, Apr. 2007.

[15] H. Prashad, "Effect of operating parameters on the threshold voltages and impedances response of non-insulated rolling element bearings under the action of electrical currents," *Wear*, vol. 117, no. 2, pp. 223–239, Jun. 1987.

[16] H. Prashad, "Appearance of craters on track surface of rolling element bearings by spark erosion," *Tribol. Int.*, vol. 34, no. 1, pp. 39–47, Jan. 2001.

[17] A. Jagenbrein, F. Buschbeck, M. Gröschl, and G. Preisinger, "Investigation of the physical mechanisms in rolling bearings during the passage of electric current," *Tribotest J.*, vol. 11, no. 4, pp. 295–306, Jun. 2005.

[18] A. Muetze, A. Binder, H. Vogel, and J. Hering, "What can bearings bear?" *IEEE Ind. Appl. Mag.*, vol. 12, no. 6, pp. 57–64, Nov./Dec. 2006.

[19] T. Zika, I. C. Gebeshuber, F. Buschbeck, G. Preisinger, and M. Gröschl, "Surface analysis on rolling bearings after exposure to defined electric stress," *Proc. IMechE J, J. Eng. Tribol.*, vol. 223, no. 5, pp. 787–797, May 2009.

[20] H. Tischmacher and S. Gattermann, "Bearing currents in converter operation," in *Proc. 14th ICEM*, Rome, Italy, Sep. 6–8, 2010, pp. 1–8.

[21] E. Wittek *et al.*, "Prediction of motor bearing currents for converter operation," in *Proc. 14th ICEM*, Rome, Italy, Sep. 6–8, 2010, pp. 1–6.

[22] A. Muetze, J. Tamminen, and J. Ahola, "Influence of motor operating parameters on discharge bearing current activity," *IEEE Trans. Ind. Appl.*, vol. 47, no. 4, pp. 1767–1777, Jul./Aug. 2011.

[23] V. Särkimäki, "Radio frequency method for detecting bearing currents in induction motors," Ph.D. dissertation, Lappeenranta Univ. Technol., Lappeenranta, Finland, 2009.

[24] J. Ahola, V. Särkimäki, A. Muetze, and J. A. Tamminen, "Radio-frequency-based detection of electrical discharge machining bearing currents," *IET Elect. Power Appl.*, vol. 5, no. 4, pp. 386–392, Apr. 2011.

[25] A. Muetze, V. Niskanen, and J. Ahola, "On radio-frequency based detection of high-frequency circulating bearing current flow," *IEEE Trans. Ind. Appl.*, vol. 50, no. 4, pp. 2592–2601, Jul./Aug. 2014.

Ville Niskanen was born in Sotkamo, Finland, in 1984. He received the M.Sc. degree in electrical engineering from Lappeenranta University of Technology (LUT), Lappeenranta, Finland, in 2010.

He is currently a Junior Researcher for proactive maintenance of electrical equipment with the Department of Electrical Engineering, LUT. His main research interests are the diagnostics of electrical-motor-driven systems.

Annette Muetze (S'03–M'04–SM'09) received the Dipl.-Ing. degree in electrical engineering from Darmstadt University of Technology, Darmstadt, Germany, in 1999, the degree in general engineering from the Ecole Centrale de Lyon, Ecully, France, in 1999, and the Dr.Tech. degree in electrical engineering from Darmstadt University of Technology in 2004.

She is a Full Professor with Graz University of Technology, Graz, Austria, where she heads the Electric Drives and Machines Institute. Prior to joining Graz University of Technology, she was an Assistant Professor with the Electrical and Computer Engineering Department, University of Wisconsin–Madison, Madison, WI, USA, and an Associate Professor with the School of Engineering, University of Warwick, Coventry, U.K.

Jero Ahola was born in Lappeenranta, Finland, in 1974. He received the M.Sc. and D.Sc. degrees in electrical engineering from Lappeenranta University of Technology (LUT), Lappeenranta, in 1999 and 2003, respectively.

He is currently a Professor of energy efficiency and preventive maintenance of electrical equipment with the Department of Electrical Engineering, LUT. His main research interests are diagnostics of electrical drive systems and power line communications.